

## The Thermal Decomposition of Lead *cyclo*-Tetraphosphate

Hiroyuki NARIAI,\* Itaru MOTOOKA, Yukio KANAJI,† and Mitsutomo TSUHAKE††

Department of Chemistry, Faculty of General Education, Kobe University, Tsurukabuto, Nada-ku, Kobe 657

†Department of Industrial Chemistry, Faculty of Engineering, Kobe University, Rokkodai-cho, Nada-ku, Kobe 657

††Kobe Women's College of Pharmacy, Kitamachi, Motoyama, Higashinada-ku, Kobe 658

(Received September 25, 1986)

The process of the thermal decomposition of lead *cyclo*-tetraphosphate dihydrate ( $P_{4m}$ ),  $Pb_2P_4O_{12} \cdot 2H_2O$ , was investigated using X-ray analysis, DTA-TG, HPLC, Isotachopheresis (IP), and IR spectrometry.  $P_{4m}$  lost water of crystallization at about 100°C. In the region of 150–170°C,  $P_{4m}$  decomposed to form oligo phosphates, and at about 190°C, oligo phosphates changed to a crystalline material which contained ortho- and triphosphate. At about 300°C, the crystalline material changed to *cyclo*-octaphosphate ( $P_{8m}$ ) through a new type of *cyclo*-tetraphosphate ( $P_{4m}^*$ ). However, in the presence of a higher water-vapor pressure than the atmospheric one, the crystalline material changed mainly to the new type of  $P_{4m}^*$  with a little  $P_{8m}$ , while at a low water-vapor pressure, the reverse tendency was observed: mainly  $P_{8m}$  and a little  $P_{4m}^*$ .

It is well-known that upon heating condensed phosphates hydrolyse or condense to form various kinds of phosphates.<sup>1–10</sup> The products obtained are pure phosphates or a mixture of linear and/or cyclic phosphates with different numbers of phosphorus atoms. These reactions are affected by the kind of metal, the degree of dryness in the crystal, the atmosphere, the temperature, and the time and rate of heating, thus resulting in the formation of different phosphates. However, these conditions have not yet been comprehensively examined.

In this work, therefore, the effect of water vapor on the thermal decomposition of lead *cyclo*-tetraphosphate ( $P_{4m}$ ) was investigated in detail. The higher-membered cyclic phosphates, such as six-membered *cyclo*-tri and eight-membered *cyclo*-tetraphosphate, are very important electrolytes because of their high negative charge on a relatively compact structure.<sup>10</sup> Schülke<sup>11</sup> reported in 1968 that  $P_{4m}$  decomposed at about 300°C to form lead *cyclo*-octaphosphate ( $P_{8m}$ ). Using metals other than lead, such as alkaline earth metals (Mg, Ca, Sr, and Ba), the present authors have investigated the thermal decompositions of *cyclo*-tetraphosphates.  $P_{8m}$  could not be obtained. Further, little is known about the detailed formation conditions; i.e., in the synthesis of  $P_{8m}$  by the method of Schülke, the product varies with the degree of the dryness of the sample used and with the method of heating. This may be attributable to the effect of water vapor in the reaction process. In this work, therefore, for the purpose of establishing the optimum conditions for the preparation of  $P_{8m}$ , the process of the thermal decomposition of  $P_{4m}$  was investigated by means of X-ray analysis, thermal analysis (DTA-TG), high-performance liquid chromatography-flow injection analysis (HPLC-FIA), Isotachopheresis (IP), and IR spectrometry.

### Experimental

**Chemicals.** The lead *cyclo*-tetraphosphate ( $P_{4m}$ ),  $Pb_2P_4O_{12} \cdot 2H_2O$ , was prepared by the method given in the literature.<sup>11</sup> Unless otherwise stated, guaranteed reagents

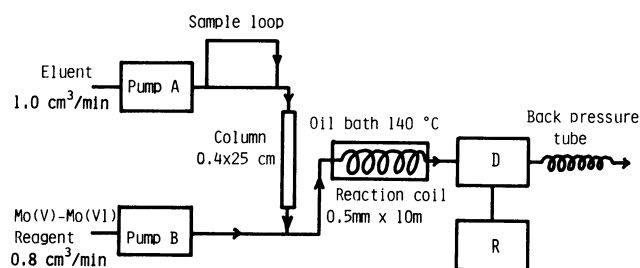


Fig. 1. Flow diagram of chromatograph and detection system. D: detector, R: recorder.

were used without further purification.

The X-ray diffraction analysis was carried out with a Rigaku Denki Geigerflex diffractometer using nickel-filtered  $Cu K\alpha$  radiation. The thermal analysis (DTA-TG) was carried out by means of a Rigaku 8002 SD thermal analyzer. The isotachopherograms were recorded on a Shimadzu IP-2A apparatus equipped with a potential gradient detector (PGD). The operational system and procedure of the isotachopheretic analysis used were as have been described previously.<sup>12–15</sup> The IR spectra were taken by means of a KBr tablet and recorded on a JASCO DS-701G Diffraction Grating Infrared Spectrophotometer.

A diagram of an HPLC-flow injection analysis (FIA) system is shown in Fig. 1. A JASCO TRIOTER V Liquid Chromatograph was used. The sample solution (100  $\mu$ l) was introduced via a loop-valve sampler onto a separation column and chromatographed at a flow-rate of 1.0  $cm^3 min^{-1}$ . The separations were performed on a column (250 $\times$ 4.0 mm I.D.) packed with a polystyrene-based anion-exchanger (TSK gel SAX,  $d_p=10 \mu m$ , Toyo Soda). The eluents for the chromatographic separation of polyphosphates were comprised of appropriate concentrations of potassium chloride and 0.1% (w/v)  $Na_4EDTA$  (pH 10). The Mo(V)–Mo(VI) reagent for the analysis of phosphates was prepared by the method of Lucena-Conde and Prat,<sup>16</sup> and was diluted 10-fold with distilled water. The diluted reagent was merged, at a flow-rate of 0.8  $cm^3 min^{-1}$ , into the stream of the column effluent. The mixed solution was then heated at 140°C in an oil bath by passing it through 10 m of 2.0 $\times$ 0.5 mm I.D. PTFE tubing. The heteropoly blue complex thus formed was detected at 830 nm in the flow cell. A back-pressure PTFE coil (1.5 m $\times$ 2.0 mm O.D. $\times$ 0.25 mm I.D.) was connected to the end coil of the flow-cell outlet to pre-

vent the formation of air bubbles on heating.<sup>17-22)</sup>

The sample solutions for HPLC-FIA was prepared as follows. Fifteen-mg portions of samples of phosphates were dissolved in 2 cm<sup>3</sup> of a 1.0 wt% sodium sulfide solution, and the lead sulfide thus precipitated was filtered out. A 1 cm<sup>3</sup> of the filtrate was diluted to 100 cm<sup>3</sup> with distilled water. A 100-μl portions of this solution was used for HPLC-FIA. The insoluble polyphosphate ( $P_{\text{high poly}}$ ) was determined in the manner described above after decomposition by heating with 3 cm<sup>3</sup> of 1.0 mol dm<sup>-3</sup> of hydrochloric acid.

The furnace used in the calcination experiments is shown in Fig. 2. The humidity in the furnace was controlled with an Ace Constant-humidity Generator Model AHC-1 (Ace Scientific Laboratory Co., Ltd.) and/or a Heatless Air Drier HF 200-9-30 (Nippon Pure Gas Co., Ltd.). The humidity of the entering air is controlled by passing the air through two water-bubbling towers maintained at the appropriate temperature to give the desired water-vapor pressure. In anhydrous experiments, the air was dried by passage through a molecular-sieve tower. The amounts of water in the dried air detected with a gas detector (GASTEC) were less than 0.1 mg dm<sup>-3</sup>.

The sample (0.1–0.2 g) was spread on the porcelain boat in a layer less than 1 mm thick to reach, almost instantly, the desired atmosphere.

## Results and Discussion

### The Thermal Decomposition by DTA-TG at Three

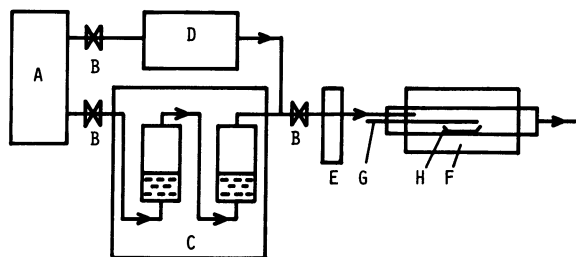


Fig. 2. Diagram of the calcination reactor. A: compressor, B: needle valve, C: constant humidity generator, D: heatless air drier, E: flow meter, F: electric furnace, G: thermocouple, H: sample boat.

**Different Atmospheres.** For the purpose of investigating the effect of water vapor upon the thermal-reaction process of  $P_{4m}$ , the heating products under atmospheric pressure, reduced pressure, and with a semi-closed cell were compared. Figure 3 shows the DTA-TG curves of  $P_{4m}$  at atmospheric pressure. Four endothermic peaks at about 100, 130, 160, and 280 °C, with a weight loss, and two exothermic peaks at about 150 and 190 °C are observed. To clarify these thermal changes at each temperature, the chromatography (HPLC) of the products at 130, 190, 260, and 335 °C, where the thermal changes were completed, was carried out. Figure 4 shows the chromatograms of the products obtained at each temperature. At 130 °C,  $P_{4m}$  lost two molecules of water of crystallization. The chromatogram at 190 °C shows that oligo phosphates such as ortho-( $P_1$ ), pyro-( $P_2$ ), tri-( $P_3$ ), and tetraphosphate( $P_4$ ) were formed; ring-opening reactions occurred at this temperature, followed by the condensation of these species to form long-chain phosphates. At 260 °C, oligo phosphates were rearranged to  $P_1$  and  $P_3$ . Perhaps, they were formed as a double salt. Schülke<sup>11)</sup> named the double salt a "crystal compound." The large peak on the chromatogram at about 53 min for the product at 335 °C indicates the formation of  $P_{8m}$ . At the same time, the amounts (peak heights) of  $P_1$  and  $P_3$  decreased with the increase in the amount of  $P_{8m}$ . The product heated at 600 °C was not dissolved in the sodium sulfide solution, indicating that insoluble polyphosphates ( $P_{\text{high poly}}$ ) were formed. As is shown in Fig. 5, the rate of the dehydration condensation reaction after ring opening under reduced pressure (about 5 Torr (1 Torr=133.322 Pa)) was faster than that under atmospheric pressure (Fig. 4), with the result that more condensed species, such as penta-( $P_5$ ), hexa-( $P_6$ ), and heptaphosphate ( $P_7$ ), was formed in an appreciable abundance. In the 260–335 °C region,  $P_{4m}$  formed again; its X-ray pattern was different from that of  $Pb_2P_4O_{12}$  prepared by dehydrating  $Pb_2P_4O_{12}$ .

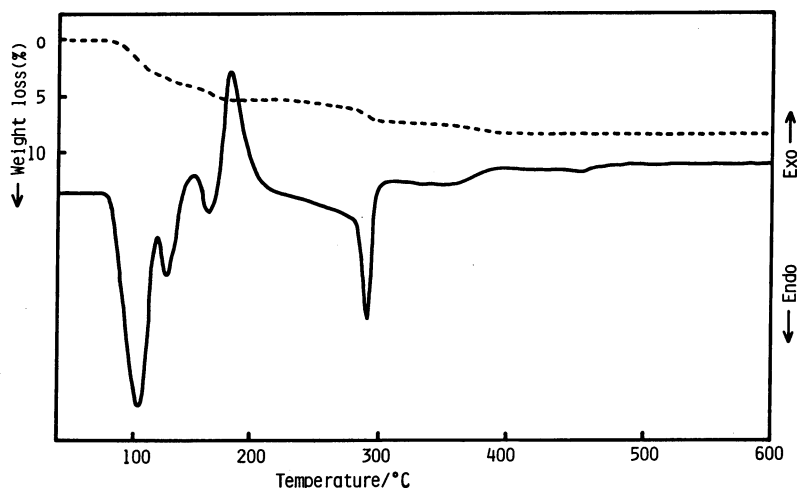


Fig. 3. DTA-TG curves of lead *cyclo*-tetraphosphate. solid line: DTA, dotted line: TG.

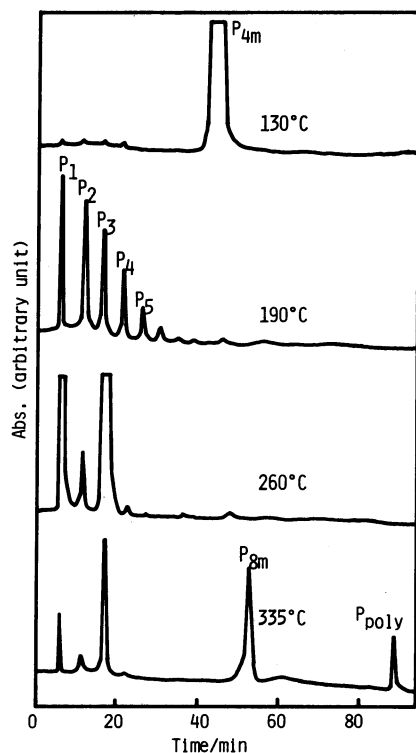


Fig. 4. Chromatograms of the products heated at several temperatures.

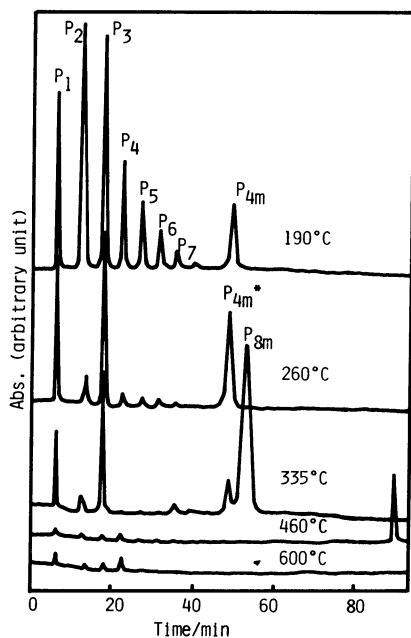


Fig. 5. Chromatograms of the products heated under reduced pressure.

2H<sub>2</sub>O.

Schülke<sup>11)</sup> reported previously that P<sub>4m</sub> formed again in this temperature range. However, the P<sub>4m</sub> species formed in the present work had another crystal structure. Further, from the IP<sup>12-15)</sup> and IR spectra<sup>23)</sup> it was confirmed that the P<sub>4m</sub> species formed in the present work was cyclic phosphate. This *cyclo*-tetraphosphate is named "high-temperature-type *cyclo*-

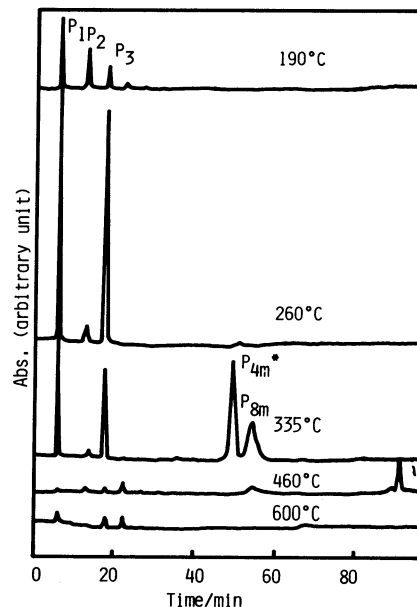


Fig. 6. Chromatograms of the products heated with semi-closed cell.

tetraphosphate (P<sub>4m</sub>\*).'' In the case of heating with a semi-closed cell, as is shown in Fig. 6, the hydrolysis proceeded rather faster than the atmospheric pressure. Even at 190°C, P<sub>4m</sub> was somewhat changed to P<sub>1</sub>, P<sub>2</sub>, and P<sub>3</sub>. P<sub>4m</sub> almost entirely turned to P<sub>1</sub> and P<sub>3</sub> at 260°C. At 335°C, P<sub>4m</sub>\* was formed, plus a small amount of P<sub>8m</sub>. Large amounts of the polyphosphates were formed at 460°C.

**Isothermal Change.** On the basis of the above results, the effect of water vapor upon the thermal decomposition of P<sub>4m</sub> was found to be significant; therefore, the influence of water vapor upon thermal decomposition was investigated by means of isothermal heating in an electric furnace at the temperatures of the respective DTA peaks. Figure 7 shows the changes in composition attributable to the calcination time of P<sub>4m</sub> at 190°C and at the relative humidities of 0 and 50%. In the case of the relative humidities of 15, 50, and 90%, approximately the same results were obtained. In the 180–200°C region, a crystalline material containing components of P<sub>1</sub> and P<sub>3</sub> (molar ratio=ca. 1:1) was formed under a 15–90% relative humidity (at 25°C). In a dry-air atmosphere (r.h.=0%), this crystalline material was changed to P<sub>4m</sub>\* (about 45% after 30 min). At 260°C, as is shown in Fig. 8, the crystalline material changed partially to P<sub>4m</sub>\* (about 45%) at a 50% relative humidity; the same results were obtained in the 15–90% range of relative humidity. However, under the dry-air conditions, both P<sub>8m</sub> and polyphosphates were produced. Moreover, insoluble polymers were formed in a considerable amount (about 70% at the maximum). This fact indicates that, under dry-air conditions, these condensation reactions proceeded more rapidly than under atmospheric conditions. When Pb<sub>2</sub>P<sub>4</sub>O<sub>12</sub> anhydride was used as the

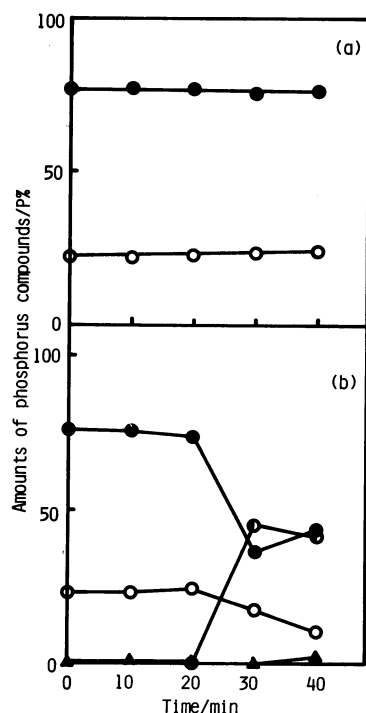


Fig. 7. The changes in composition with calcination time of  $\text{Pb}_2\text{P}_4\text{O}_{12} \cdot 2\text{H}_2\text{O}$  at  $190^\circ\text{C}$  and at various relative humidities. (a): 50%, (b): 0%, —○—:  $\text{P}_1$ , —△—:  $\text{P}_2$ , —●—:  $\text{P}_3$ , —●—:  $\text{P}_{4m}^*$ .

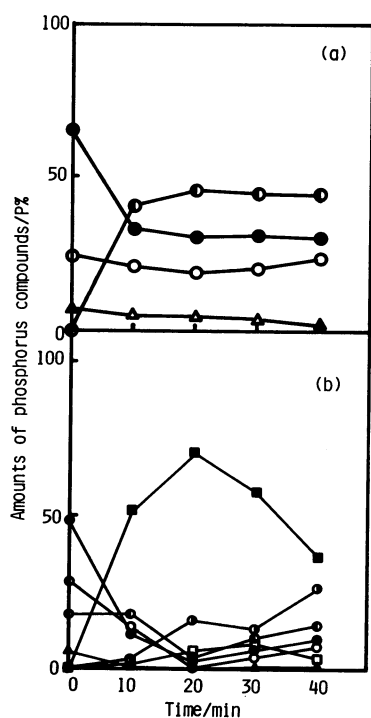


Fig. 8. The changes in composition with calcination time of  $\text{Pb}_2\text{P}_4\text{O}_{12} \cdot 2\text{H}_2\text{O}$  at  $260^\circ\text{C}$  and at various relative humidities. (a): 50%, (b): 0%, —○—:  $\text{P}_1$ , —△—:  $\text{P}_2$ , —●—:  $\text{P}_3$ , —●—:  $\text{P}_{4m}^*$ , —●—:  $\text{P}_{8m}$ , —□—:  $\text{P}_{\text{poly}}$ , —■—:  $\text{P}_{\text{high poly}}$ .

starting material, similar results were obtained. Therefore, the crystalline material was formed at  $260^\circ\text{C}$ ,

Table 1. Changes in the Amounts of Phosphorus Compounds in the Samples Heated at  $250^\circ\text{C}$  at Various Relative Humidities (r.h.) for 40 min (with a crystalline material containing components of  $\text{P}_1$  and  $\text{P}_3$  as the starting material)

Compound (r.h., %)	$\text{P}_1$ %	$\text{P}_2$ %	$\text{P}_3$ %	$\text{P}_{4m}^*$ %	$\text{P}_{8m}$ %	$\text{P}_{\text{oligo}}$ %
0	20.0	4.0	29.4	35.7	10.3	0.6
15	16.0	3.3	37.5	42.8	0	0.4
50	17.3	3.2	37.9	40.6	0	1.0
90	11.9	5.0	52.5	29.0	0	1.6

Table 2. Changes in the Amounts of Phosphorus Compounds in the Samples Heated at  $280^\circ\text{C}$  at Various Relative Humidities (r.h.) for 40 min (with a crystalline material containing components of  $\text{P}_1$  and  $\text{P}_3$  as the starting material)

Compound (r.h., %)	$\text{P}_1$ %	$\text{P}_2$ %	$\text{P}_3$ %	$\text{P}_{4m}^*$ %	$\text{P}_{8m}$ %	$\text{P}_{\text{oligo}}$ %
0	0	0	2.8	5.7	89.3	2.2
15	8.0	1.4	24.2	28.5	37.9	0
50	7.9	0.7	23.9	32.6	34.9	0
90	14.0	3.9	34.0	43.0	4.1	1.0

regardless of the starting material. In the dry-air atmosphere, even at  $200^\circ\text{C}$ ,  $\text{P}_{4m}^*$  was already formed in an amount of 46%. As has been mentioned above, a crystalline material containing components of  $\text{P}_1$  and  $\text{P}_3$  was formed at about  $200^\circ\text{C}$  by means of an exothermic reaction. Whatever the starting material ( $\text{Pb}_2\text{P}_4\text{O}_{12} \cdot 2\text{H}_2\text{O}$  or  $\text{Pb}_2\text{P}_4\text{O}_{12}$ ), the crystalline material was formed. To clarify the effect of the water content in the heating atmosphere at the second endothermic peak, the process of the formation of  $\text{P}_{8m}$  was investigated using the crystalline material which had been prepared by heating  $\text{Pb}_2\text{P}_4\text{O}_{12} \cdot 2\text{H}_2\text{O}$  at  $200^\circ\text{C}$  for 40 min in an electric furnace. Table 1 shows the changes in the amounts of phosphorus compounds in the samples heated at  $250^\circ\text{C}$ . At  $250^\circ\text{C}$ , a temperature before the endothermic peak (Fig. 3), we expected a remarkable effect of the water vapor upon the formation of  $\text{P}_{8m}$ . In the dry-air atmosphere (0%), the amounts of  $\text{P}_1$  and  $\text{P}_3$  decreased,  $\text{P}_{4m}^*$  was formed, and  $\text{P}_{8m}$  was obtained in about a 10% yield. However, in a 15–90% relative-humidity atmosphere (at  $25^\circ\text{C}$ ),  $\text{P}_{4m}^*$  increased with the decrease in  $\text{P}_1$  and  $\text{P}_3$ , while  $\text{P}_{8m}$  was not formed at all. Further, at  $280^\circ\text{C}$  and at a 0% relative humidity atmosphere, as is shown in Table 2, the amount of  $\text{P}_{8m}$  reached about 90%, and at a 15–50% relative humidity (at  $25^\circ\text{C}$ ), that of  $\text{P}_{8m}$ , 35–38%. In the dry-air atmosphere,  $\text{P}_1$  and  $\text{P}_3$  decreased, while, in turn,  $\text{P}_{4m}^*$  was formed, followed by the formation of  $\text{P}_{8m}$  in fairly large quantities. However, in a 90% relative humidity,  $\text{P}_1$  and  $\text{P}_3$  remained in fairly large quantities, resulting

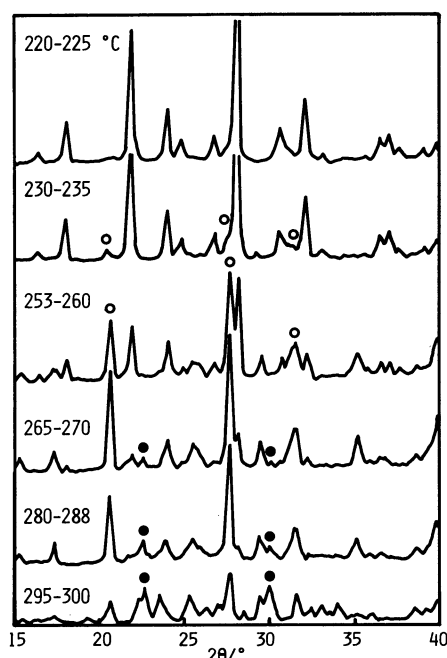
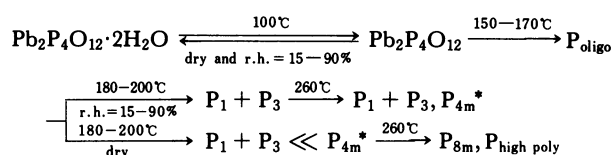


Fig. 9. X-Ray diffraction patterns of products on heating. ○:  $P_{4m}^*$ , ●:  $P_{8m}$ .

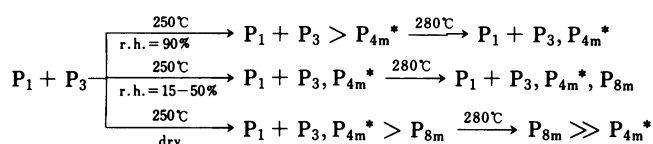
in the formation of  $P_{4m}^*$  in a large quantity, and a little  $P_{8m}$  was formed.

The process of the thermal decomposition of lead *cyclo*-tetraphosphate under several humid atmospheres may be summarized schematically as follows:

1)  $Pb_2P_4O_{12} \cdot 2H_2O$  as the starting material.



2)  $P_1 + P_3$  as the starting material.



$P_1 + P_3$ : crystalline material. The symbols  $>$  and  $\gg$  show the quantitative relations between the products.

**X-Ray Analysis on Heating  $P_{4m}^*$ .** In order to clarify the facts presented above, X-ray measurements were performed. Figure 9 shows the X-ray diffraction patterns of  $Pb_2P_4O_{12} \cdot 2H_2O$  at several stages of heating in an electric furnace attached to the X-ray diffractometer. In the 200–225°C region,  $P_1$  and  $P_3$  remained unchanged. At 230–235°C, the characteristic diffraction lines of  $P_{4m}^*$  at  $2\theta = 20.6$  and  $27.7^\circ$  began to appear; they gradually increased with the heating temperature. The X-ray diffraction pattern at 265–270°C showed  $P_{4m}^*$ , the diffraction lines of  $P_1$  and  $P_3$

became very small, and small peaks of  $P_{8m}$  began to appear. At 280–288°C, the peaks of  $P_1$  and  $P_3$  disappeared and  $P_{4m}^*$  began to form (or the peaks of  $P_{4m}^*$  began to be recognized). At the same time, the peaks of  $P_{8m}$  also increased. At 295–300°C, the peaks of the diffraction pattern are those of  $P_{4m}^*$  and  $P_{8m}$ . The peaks of  $P_{8m}$  appeared distinctly with the temperature. These results confirmed that the crystalline material changes to  $P_{8m}$  through  $P_{4m}^*$ . The optimum conditions for preparing  $P_{8m}$  are as follows. It is desirable to have a low water-vapor pressure when  $P_1$  and  $P_3$  condense to  $P_{8m}$  through a new type,  $P_{4m}^*$ , at about 300°C.

The authors wish to thank Mr. Nobuyuki Tada for his helpful work.

#### References

- 1) S. L. Friess, *J. Am. Chem. Soc.*, **74**, 4027 (1952).
- 2) J. D. McGilvery and A. E. Scott, *Can. J. Chem.*, **32**, 1100 (1954).
- 3) J. R. Van Wazer and E. Karl-Kroupa, *J. Am. Chem. Soc.*, **78**, 1772 (1956).
- 4) J. F. McCullough, J. R. Van Wazer, and E. J. Griffith, *J. Am. Chem. Soc.*, **78**, 4528 (1956).
- 5) R. P. Langguth, R. K. Osterheld, and E. Karl-Kroupa, *J. Phys. Chem.*, **60**, 1335 (1956).
- 6) E. Thilo and U. Schülke, *Z. Anorg. Allg. Chem.*, **341**, 293 (1965).
- 7) E. J. Griffith and R. L. Buxton, *Inorg. Chem.*, **4**, 549 (1965).
- 8) M. Watanabe, S. Sato, and H. Saito, *Bull. Chem. Soc. Jpn.*, **48**, 896 (1975).
- 9) M. Watanabe, M. Matsuura, and T. Yamada, *Bull. Chem. Soc. Jpn.*, **54**, 738 (1981).
- 10) G. Kura, *Bull. Chem. Soc. Jpn.*, **56**, 3769 (1983).
- 11) U. Schülke, *Z. Anorg. Allg. Chem.*, **360**, 231 (1968).
- 12) T. Yagi, K. Kojima, H. Nariai, and I. Motooka, *Bull. Chem. Soc. Jpn.*, **55**, 1831 (1982).
- 13) H. Nariai, K. Nakazaki, M. Tsuchiko, and I. Motooka, *J. Chromatogr.*, **248**, 135 (1982).
- 14) I. Motooka, H. Nariai, K. Nakazaki, and M. Tsuchiko, *J. Chromatogr.*, **260**, 377 (1983).
- 15) I. Motooka, H. Nariai, K. Nakazaki, and M. Tsuchiko, *J. Chromatogr.*, **295**, 533 (1984).
- 16) F. Lucena-Conde and L. Prat, *Anal. Chim. Acta*, **16**, 473 (1957).
- 17) Y. Hirai, N. Yoza, and S. Ohashi, *Anal. Chim. Acta*, **115**, 269 (1980).
- 18) Y. Hirai, N. Yoza, and S. Ohashi, *Bunseki Kagaku*, **30**, 465 (1981).
- 19) Y. Baba, N. Yoza, and S. Ohashi, *J. Chromatogr.*, **318**, 319 (1985).
- 20) Y. Baba, N. Yoza, and S. Ohashi, *J. Chromatogr.*, **348**, 27 (1985).
- 21) Y. Baba, N. Yoza, and S. Ohashi, *J. Chromatogr.*, **350**, 119 (1985).
- 22) Y. Baba, N. Yoza, and S. Ohashi, *J. Chromatogr.*, **350**, 461 (1985).